



# Kinetic study of heating pinewood sawdust with different methods using thermogravimetric analysis

Francisco Márquez-Montesino<sup>1</sup> · Fernando Trejo<sup>2</sup> · José Guadalupe Rutiaga-Quiñones<sup>3</sup> · Fermín Correa-Méndez<sup>4</sup>

Received: 14 November 2020 / Accepted: 17 February 2021 / Published online: 5 March 2021  
© Akadémiai Kiadó, Budapest, Hungary 2021

## Abstract

A kinetic study based on pinewood (*Pinus montezumae*) was carried out at heating rates of 5, 10, 15, and 20 °C min<sup>-1</sup>. The Flynn–Wall–Ozawa (FWO), Kissinger–Aka-hira–Sunose (KAS), and Friedman methods were used to analyze the thermal behavior of samples. Thermogravimetry (TG) and derivative thermogravimetry (DTG) curves were obtained at non-isothermal conditions. Ultimate and proximate analyzes from pinewood were obtained and the greater decomposition was in the range of 250 to 380 °C. Mean values of activation energy ( $E_a$ ) and frequency factor ( $A$ ) by FWO method were 192.4 kJ mol<sup>-1</sup> and  $2.73 \times 10^{14}$  min<sup>-1</sup>, respectively, whereas the aforementioned values by KAS method were 181.8 kJ mol<sup>-1</sup> and  $3.32 \times 10^{13}$  min<sup>-1</sup>. Lower value of mean activation energy (174.1 kJ mol<sup>-1</sup>) was obtained with Friedman method.

**Keywords** Isoconversional method · Lignocellulosic materials · Pyrolysis kinetics · Thermogravimetric analysis

## Greek letters

$\alpha$  [-] Normalized conversion  
 $\beta$  [°C min<sup>-1</sup>] Heating rate

---

✉ Fernando Trejo  
ftrejoz@ipn.mx

<sup>1</sup> Departamento de Química, Universidad de Pinar del Río, C.P. 20100 Pinar del Río, Cuba

<sup>2</sup> Instituto Politécnico Nacional, CICATA-Legaria, Legaria 694, Col. Irrigación, 11500 Mexico City, Mexico

<sup>3</sup> Facultad de Ingeniería en Tecnología de la Madera, Edificio D, Ciudad Universitaria, Universidad Michoacana de San Nicolás de Hidalgo, Av. Fco. J. Múgica s/n, Col. Felicitas del Río, 58040 Morelia, Michoacán, Mexico

<sup>4</sup> Programa Académico Desarrollo Sustentable, Universidad Intercultural Indígena de Michoacán, Carretera San Juan Tumbio-Cheran, km 16.2, CP 60291 Pátzcuaro, Estado de Michoacán, Mexico

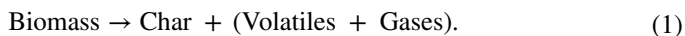
## Abbreviations

A [ $s^{-1}$ or $min^{-1}$ ]	Frequency factor
B [ $^{\circ}C\ min^{-1}$ ]	Heating rate
$E_a$ [ $kJ\ mol^{-1}$ ]	Activation energy
HHV [ $MJ\ kg^{-1}$ ]	Higher heating value
K [ $s^{-1}$ or $min^{-1}$ ]	Kinetic constant
$m_f$ [mg]	Final mass
$m_i$ [mg]	Initial mass
$m_t$ [mg]	Mass at any time
n [-]	Reaction order
R [ $kJ\ mol^{-1}\ K^{-1}$ ]	Gas constant
T [K]	Absolute temperature
t [s]	Time
$T_{\alpha}$ [K]	Absolute temperature at which top conversion is achieved
X [-]	Conversion
Z [ $s^{-1}$ ]	Average frequency factor

## Introduction

Pyrolysis of biomass occurs at different heating rates by which it is classified as slow, fast, flash, and reactive pyrolysis [1–3]. Inert atmosphere is required to accomplish the pyrolysis reaction and gas, liquid or solid products are obtained depending on the heating rates at which reaction takes place. In addition, temperature, pressure, reaction time, moisture, composition, and particle size must be also considered [4]. Thermogravimetric analysis (TG) is commonly used to study the devolatilization kinetics and it has been found that wood decomposition mainly ranged from 250 to 350 °C in which hemicellulose is converted while cellulose is almost fully transformed through breakage of glycosidic bonds [5]. Devolatilization of poplar wood ranged from 177 to 467 °C as reported elsewhere [4]. For wood soot, values were reported to be 200–500 °C [6] while devolatilization of *Acacia mangium* ranged from 250 to 380 °C [7]. For pine sawdust, the range was 200–400 °C [8] and 210–390 °C for *Pynion* pine [9]. Studies on non-edible seeds of Mahua, Karanja, Niger, and Linseed showed wider intervals of devolatilization from 200 to 500 °C [10]. In all reports, it has been considered that thermal decomposition of biomass considers three stages: (1) dehydration, where water and volatiles are lost at temperature lower than 200 °C, (2) hemicellulose and cellulose decomposition, and (3) lignin decomposition that include a wide range of temperature.

Thermochemical conversion requires knowing properties and kinetics of biomass where heating rate, feed, and atmosphere are needed to calculate the activation energy and frequency factor [11, 12]. Commonly, thermal decomposition of biomass is expressed as follows [13, 14]:



The kinetic expression that describes this process is written as follows:

$$\frac{d\alpha}{dt} = k(T)f(\alpha). \quad (2)$$

Here  $t$  is time,  $k(T)$  is the kinetic constant as function of temperature,  $f(\alpha)$  is a function depending on the reaction mechanism,  $\alpha$  is the normalized conversion, which in turn is defined as follows [9, 12, 15, 16]:

$$\alpha = \frac{m_i - m_t}{m_i - m_f}. \quad (3)$$

Here  $m_i$  is the initial mass (in mg),  $m_f$  is the final mass (in mg) at the maximum temperature,  $m_t$  is the mass (in mg) at any time. The kinetic constant is given by the Arrhenius equation as:

$$k(T) = Ae^{-\left(\frac{E_a}{RT}\right)}. \quad (4)$$

$A$  is the frequency factor given ( $\text{imin}^{-1}$ ),  $E_a$  is the activation energy ( $\text{kJ mol}^{-1}$ ),  $R$  is the gas constant to be  $8.314 \text{ J mol}^{-1} \text{ K}^{-1}$  and  $T$  is absolute temperature (in K). By substituting Eq. 4 into Eqs. 2, 5 is obtained to describe the dependence of the kinetic constant on temperature [4, 10, 17, 18]:

$$\frac{d\alpha}{dt} = -Ae^{-\left(\frac{E_a}{RT}\right)}f(\alpha). \quad (5)$$

Based on reaction kinetics,  $f(\alpha)$  is written as follows:

$$f(\alpha) = (1 - \alpha)^n. \quad (6)$$

Here  $(1 - \alpha)$  is the remaining solid fraction, which is still able to be converted, and  $n$  is the reaction order.

By substitution of Eq. 6 into Eq. 5, the following reaction rate is obtained:

$$\frac{d\alpha}{dt} = -Ae^{-\left(\frac{E_a}{RT}\right)}(1 - \alpha)^n. \quad (7)$$

Several non-isothermal methods based on thermogravimetry have been reported in literature, [4, 8, 19, 20] which can be divided into two types: (1) model-based kinetics, and (2) model-free kinetics or isoconversional methods. Model-based kinetics use models to fit data and one of them is chosen when the best statistical behavior is achieved. Isoconversional or model-free methods do not require a mathematical model. Instead, several curves at different heating rates are used to calculate kinetic parameters at the same conversion value and obtaining its activation energy value. Activation energies at different conversion values give a profile as function of conversion. Different approaches based on isoconversional models are used such as the Friedman, Flynn–Wall–Ozawa, and Kissinger–Akahira–Sunose methods.

### Friedman method

Particularly, the Friedman method is the most common one among them where changes in conversion as function of temperature is obtained. This model does not require to know the reaction model and it is represented as follows once natural logarithm is applied:

$$\ln\left(\frac{dX}{dt}\right) = \ln A + n \ln(1 - X) - \frac{E_a}{RT}. \quad (8)$$

Using this equation, the activation energy is determined by plotting  $\ln(dX/dt)$  against  $1/T$  to obtain a group of parallel lines having  $-E_a/R$  as slope [20, 21]. The interception term defined as  $\ln[nA(1-X)]$  is calculated from the parallel lines for each conversion value at each heating rate.

### Flynn–Wall–Ozawa (FWO) method

The Flynn–Wall–Ozawa method is widely accepted as well as the Friedman method to calculate kinetic parameters when thermal studies are carried out. The model is represented as follows [22, 23]:

$$g(\alpha) = \int_0^\alpha \frac{d\alpha}{f(\alpha)} = \frac{A_\alpha}{\beta_i} \int_0^T \exp\left(-\frac{E_\alpha}{RT_{\alpha i}}\right) dT_{\alpha i} = \frac{A_\alpha E_\alpha}{\beta_i R} P(u). \quad (9)$$

In this method, it is considered that  $A_\alpha$ ,  $\alpha$ , and  $E_\alpha$  are independent of temperature. By taking logarithms the equation is transformed into:

$$\ln[g(\alpha)] = \ln\left(\frac{A_\alpha E_\alpha}{R}\right) - \ln \beta_i + \ln[P(u)]. \quad (10)$$

Using the Doyle's approach, the following term is attained:

$$\ln[P(u)] \approx -5.331 - 1.052 \frac{E_\alpha}{RT_{\alpha i}}. \quad (11)$$

Finally, the model based on FWO method is:

$$\ln(\beta_i) = \ln\left(\frac{A_\alpha E_\alpha}{Rg(\alpha)}\right) - 5.331 - 1.052 \frac{E_\alpha}{RT_{\alpha i}}. \quad (12)$$

Here  $g(\alpha)$  is constant at a given conversion value. Subscripts  $i$  and  $\alpha$  correspond to the heating rate and conversion, respectively [4, 11, 16, 20, 24, 25].

If the heating rate ( $\beta_i$ ) is fixed, then the activation energy is obtained from the slope of the last equation when plotting  $\ln(\beta_i)$  against  $1/T_{\alpha i}$  at different conversion values.

## Kissinger–Akahira–Sunose (KAS) method

In the KAS method, assumptions are similar to FWO method. The difference among them is the P(u) approach. In this case, it is equated to [13, 22]:

$$\ln [P(u)] \approx \frac{e^{-u}}{u^2}, \quad (13)$$

$$\text{if } u = \frac{E_\alpha}{RT_{\alpha i}}. \quad (14)$$

Then Eq. 10 takes the following form:

$$\ln \left( \frac{\beta_i}{T_{\alpha i}^2} \right) = \ln \left( \frac{A_\alpha R}{E_\alpha g_\alpha} \right) - \frac{E_\alpha}{RT_{\alpha i}}. \quad (15)$$

In this method, the knowledge of the thermal decomposition mechanism is not required. Apparent activation energy is obtained through plotting  $\ln(\beta_i)/T_{\alpha i}^2$  versus  $1000/T_{\alpha i}$ . For a given conversion value ( $\alpha$ ), the slope is  $-E_\alpha/R$  in the range from 0 to 1.

## Calculation of the frequency factor

Most of studies based on thermal analysis have been carried out at constant heating rate [11, 22, 24]. In addition, Lyon [26] reported a useful solution for the constant heating rate Arrhenius integral by which isoconversional equation is obtained to calculate the activation energy and frequency factor without knowing the form of the rate law as follows:

$$Z = \frac{B(E_\alpha + 2RT_\alpha)e^{E_\alpha/RT_\alpha}}{RT_\alpha^2}. \quad (16)$$

Here  $B$  is the heating rate in  $^\circ\text{C min}^{-1}$ ,  $T_\alpha$  is the absolute temperature at which the top conversion is achieved. Using Eq. 9 is an alternative way to calculate the frequency factor.

Considering these approaches, the aim of this study is to calculate the kinetic parameters using the FWO, KAS, and Friedman methods on *Pinus montezumae* sawdust. A comparison of activation energies among the three methods was carried out.

## Materials and methods

### Characterization of samples

Chips around 1 mm of pine wood (*Pinus montezumae*) from the Mexican State of Michoacan were used. Previously, the wood was dried at 110  $^\circ\text{C}$  during 12 h up to

constant mass. Characterization of the feed was carried out following the ASTM and TAPPI standards. Lignin was determined according to ASTM D1106-96 standard [27]. Cellulose was quantified by TAPPI T 203 cm-99 method [28]. Hemicellulose was determined by ASTM D1104-56 method [29]. Proximate analysis to determine moisture content, ash, and volatile matter were quantified by ASTM D4442-16 [30], ASTM D1102-84 [31] and ASTM D3175-18 [32] standards, respectively, whereas ultimate analysis was carried out by weighing 2 mg in a Perkin Elmer elemental analyzer model 2400 to determine C, H, O, and N. Elemental analysis was done by triplicate and the average values is reported.

### Kinetics and thermogravimetric analysis

Non-isothermal thermogravimetric analysis was carried out in a TA Instruments thermobalance model Q5000 to measure the variations in mass as function of time. Kinetic study was carried out under nitrogen atmosphere at  $50 \text{ cm}^3 \text{ min}^{-1}$ . Sample was heated up to  $800 \text{ }^\circ\text{C}$  at different heating rates, i.e., 5, 10, 15, and  $20 \text{ }^\circ\text{C min}^{-1}$  to register variations in mass and temperature as function of time [33–37] while the reaction order was assumed to be  $n=1$ . Other authors have demonstrated that linear regression of Arrhenius equation is better represented when reaction order is  $n=1$  during biomass pyrolysis [38, 39]. Model-free methods such as Flynn–Ozawa–Wall (FWO) and Kissinger–Akahira–Sunose (KAS) were used as well as the Friedman method. Seven conversion values ( $\alpha$ ) from 20 to 80% were used.

## Results and discussion

### Characterization of samples

Table 1 shows the proximate and ultimate analyzes as well as composition of pine wood. Lignin and fixed carbon average contents are 29.23 wt% and 6.26 wt%, respectively. Hemicellulose is obtained as the summation of hemicellulose and cellulose contents as reported elsewhere and, in this case, it accounts to be 70.77 wt%. Moghadam [40] reported contents of lignin and fixed carbon of 59.3 and 48.5 wt%, respectively, for palm kernel shell while similarities in composition can be found in other reports using pine sawdust, hazelnut husk and *Acacia mangium* wood [7, 25]. Proximate analysis shows the high content of volatile matter that consist of light hydrocarbons and tars. Oxygen content is also high as demonstrated by ultimate analysis, which indicates the presence of polysaccharides such as cellulose and hemicellulose [41].

### Thermogravimetric analysis

Devolatilization of lignocellulosic materials involves decomposition of cellulose, hemicellulose, and lignin. According to Fig. 1, the highest degradation occurred

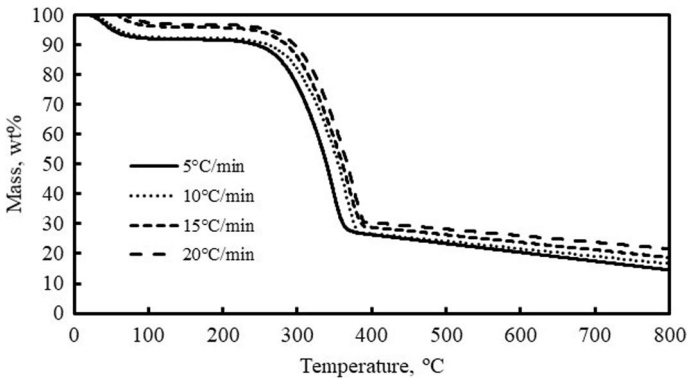


**Fig. 1** TG profiles for *Pinus montezumae* wood at 5, 10, 15, and 20 °C min<sup>-1</sup> under nitrogen atmosphere at 50 cm<sup>3</sup> min<sup>-1</sup>. Temperature ranged from ambient to 800 °C

**Table 1** Characterization of *Pinus montezumae* wood

Property	Proximate analysis, wt%
Moisture	6.80 ± 0.27
Ash	0.40 ± 0.02
Volatile matter	86.54 ± 2.60
Fixed carbon	6.26 ± 0.25
	Ultimate analysis, wt%
C	49.40 ± 0.97
H	5.91 ± 0.12
N	0.15 ± 0.01
O	44.54 ± 0.89
	Composition, wt%
Hemicellulose	16.30 ± 0.32
Cellulose	54.47 ± 1.08
Lignin	29.23 ± 0.58

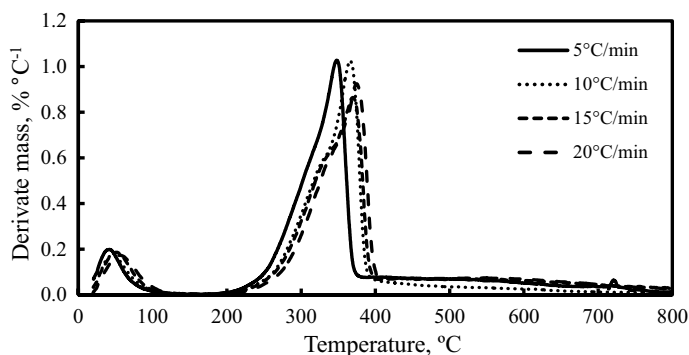
between 250 and 350 °C. Three stages are observed, i.e., the first one comprises from 90 to 250 °C in which water and volatiles on material surface are lost; the second stage starts at 250 °C with decomposition of biomass and releasing CO, CO<sub>2</sub> and volatile compounds as by-products due to degradation of hemicellulose, cellulose, and lignin that conform the pine wood. From 380 °C, biomass is mostly decomposed to yield fixed carbon residue. Lignin is an amorphous polymer whose degradation is carried out in wide range even at higher temperature than 400 °C by which steadily mass loss is observed over this value. This is likely due to deposition of carbon formed from hemicellulose and cellulose [9, 42]. At higher temperature, the mass loss of this residue is observed since secondary reactions involving polymerization and condensation [12, 43, 44].

Fig. 2 shows the peaks at which the highest thermal degradation was carried out. Displacement to the right is observed due to heat transfer limitations. At lower heating rate, the energy given to the sample is higher and more time is necessary to reach the equilibrium between the gas carrier and the furnace. At the same time and temperature, but at higher heating rate, the reaction time is shorter, and temperature needed for sample decomposition is also higher as reported elsewhere on nutshells, poplar wood and *Pynion* pine [4, 9, 45]. Separation of peaks of hemicellulose and cellulose are not clearly because of partial overlapping of both processes during thermal degradation. For this reason, a shoulder is observed in all peaks around 300–340 °C. The peak located at lower temperatures is attributed to hemicellulose while the highest one corresponds to cellulose. Lignin is decomposed in a wider interval of temperatures [9, 12, 13, 21, 46–48].

It is to be considered that *Pinus montezumae* sawdust utilized in this study has a lower moisture content (average value of 6.80 wt%) by which this biomass could be potentially used as feedstock in thermochemical conversion processes such as gasification. In addition, the high volatile matter content implies high reactivity by gas releasing during pyrolysis reaction by which gas–gas reaction rates are improved [49]. The higher heating value of the biomass may be calculated as follows [50]:

$$HHV = 0.3491 \times C + 1.1783 \times H + 0.1005 \times S - 0.1034 \times O - 0.0151 \times N - 0.0211 \times \text{Ash content}. \quad (17)$$

Here C, H, S, O, and N are the ultimate analysis values, and ash content is obtained from proximate analysis as shown in Table 1. In this case, sulfur was not detected, and its content is neglected. According to Eq. 17, the HHV of *Pinus montezumae* is 19.59 MJ kg<sup>-1</sup>, which can be considered as suitable to produce renewable fuels through thermal conversion processes.



**Fig. 2** DTG profiles for *Pinus montezumae* wood at 5, 10, 15, and 20 °C min<sup>-1</sup> under nitrogen atmosphere at 50 cm<sup>3</sup> min<sup>-1</sup>. Temperature ranged from ambient to 800 °C



## Kinetic analysis

When using thermogravimetric methods for studying pyrolysis kinetics of different raw sources including biomass like forest residues, a variation of activation energy as function of conversion is attained, which means that pyrolysis of pine sawdust proceeds through multiple-stage kinetics where several thermal reactions are affected by changes in heating rate. Particularly, the so-called model-free methods consider that the reaction extent is constant by which the reaction rate depends on temperature. In addition, if activation energy is the main variable, the knowledge of reaction mechanism is not required [22]. However, during conversion of pine sawdust the  $E_a$  values change as reaction progresses. Differences in activation energy is due to variations in composition and amount of hemicellulose, cellulose, and lignin. Transformations of these constituents follow different reaction mechanisms and different values of activation energy as conversion proceed.

To determine the kinetic parameters, plots of  $\ln(\beta)$  versus  $1000/T$  in  $K^{-1}$  and  $\ln(\beta_i/T_{ai}^2)$  versus  $1000/T_{ai}$  in  $K^{-1}$  for the FWO and KAS methods, respectively, were depicted as shown in Fig. 3a and b. Fractional conversion was studied from 0.2 to 0.8

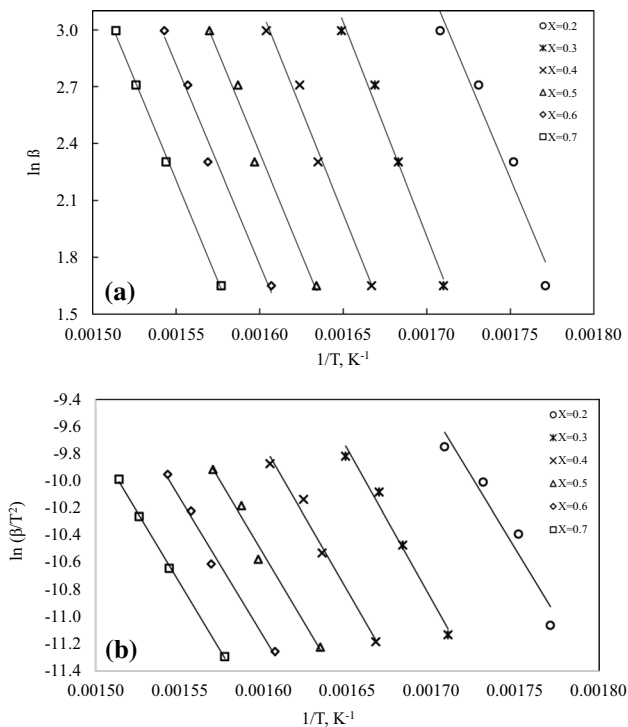


**Fig. 3** Kinetic calculations for **a** FWO and **b** KAS methods based on variable heating rates, i.e., 5, 10, 15, and 20  $^{\circ}C\ min^{-1}$  under nitrogen atmosphere at 50  $cm^3\ min^{-1}$ . Fractional conversion plotted was in the range from 0.2 to 0.7

**Table 2** Activation energy calculated from TG by FWO and KAS methods at different conversion values

X	FWO method			KAS method		
	Ea, kJ mol <sup>-1</sup>	Equation	R <sup>2</sup>	Ea, kJ mol <sup>-1</sup>	Equation	R <sup>2</sup>
0.2	178.9 ± 3.6	y = -21520x + 39.859	0.9427	169.3 ± 3.3	y = -20365x + 25.141	0.9365
0.3	193.4 ± 3.9	y = -23265x + 41.436	0.9830	183.4 ± 3.6	y = -22060x + 26.634	0.9812
0.4	188.3 ± 3.8	y = -22651x + 39.381	0.9839	178.1 ± 3.5	y = -21425x + 24.544	0.9820
0.5	183.2 ± 5.5	y = -22038x + 37.598	0.9838	172.9 ± 5.2	y = -20795x + 22.733	0.9818
0.6	180.9 ± 5.4	y = -21754x + 36.535	0.9873	170.2 ± 5.1	y = -20467x + 21.602	0.9858
0.7	182.2 ± 7.3	y = -21920x + 36.166	0.9993	171.4 ± 6.8	y = -20615x + 21.205	0.9991
0.8	239.9 ± 9.6	y = -28860x + 40.585	0.8919	227.5 ± 9.1	y = -27360x + 25.345	0.8813
Average	192.4			181.8		

0.8 because poor correlation is obtained at values lower than 0.2 and higher than 0.8. Apparent activation energies were obtained from the slope in Fig. 3a and b and tabulated in Table 2 as well as determination coefficients. In addition, equations describing the conversion process are also summarized. Frequency factors were calculated according to Eq. 16 and shown in Table 3 at different heating rates. It is observed that apparent activation energy differs as function of conversion in both methods. It has been reported that complex mechanisms occur due to decomposition of lignin, which is a branched and mainly amorphous polymer constituted by phenylpropane units [4, 51]. Thermal degradation of lignin is carried out in a wider range of temperatures to form carbohydrate derivatives, syringyl, guaiacyl, and modified lignin. In addition, carbohydrate derivatives undergo rearrangements while guaiacyl and syringyl are the mainly prevalent units [52]. On the other hand, hemicellulose and cellulose decompose faster than lignin in the intervals of 200–300 °C and 300–340 °C, respectively [53].

The increase of activation energy when varying fractional conversion from 0.2 to 0.3 as shown by FWO and KAS methods may be associated to endothermic reactions, such as elimination of moisture and adsorbed gases. Then a decrease of activation energy from 0.4 to 0.6 is related to exothermic reactions involving lignin decomposition occurred by scission of aliphatic groups followed by degradation of aromatic rings. The fast increasing in the activation energy from lower to mid fractional conversion values (0.1–0.6) was attributed to endothermic reactions [14] while exothermic reactions were observed from mid to high conversions (0.6–0.8). When lignocellulosic are pyrolyzed, the cleavage of C–O aromatic bonds in lignin forms products having a single oxygen atom while methoxy C–O bonds forms compounds with two-oxygen atoms [54]. Further increase from 0.7 to 0.8 also raises the activation energy very sharp due to mainly lignin fraction is carbonized having graphite-like structures formed through endothermal processes.

The average activation energies calculated from FWO and KAS methods were 192.4 and 181.8 kJ mol<sup>-1</sup>, respectively, whereas the average frequency factor for heating rate of 5 °C min<sup>-1</sup>, is  $2.73 \times 10^{14}$  and  $3.32 \times 10^{13}$  min<sup>-1</sup> for the FWO and KAS methods, respectively. As observed from Table 3, frequency factors calculated

**Table 3** Frequency factor (*Z*) calculated at different heating rates ( $\beta$ ) from activation energy obtained by FWO and KAS methods at different conversion values (*X*)

<i>X</i>	$\beta = 5\text{ }^\circ\text{C min}^{-1}$		$\beta = 10\text{ }^\circ\text{C min}^{-1}$		$\beta = 15\text{ }^\circ\text{C min}^{-1}$		$\beta = 20\text{ }^\circ\text{C min}^{-1}$	
	FWO	KAS	FWO	KAS	FWO	KAS	FWO	KAS
0.2	$2.09 \times 10^{14} \pm 4.18 \times 10^{12}$	$2.57 \times 10^{13} \pm 5.14 \times 10^{11}$	$2.73 \times 10^{14} \pm 5.46 \times 10^{12}$	$3.42 \times 10^{13} \pm 6.84 \times 10^{11}$	$2.55 \times 10^{14} \pm 5.10 \times 10^{12}$	$3.28 \times 10^{13} \pm 6.56 \times 10^{11}$	$2.02 \times 10^{14} \pm 4.04 \times 10^{12}$	$2.67 \times 10^{13} \pm 5.34 \times 10^{11}$
0.3	$1.14 \times 10^{15} \pm 2.28 \times 10^{13}$	$1.37 \times 10^{14} \pm 2.74 \times 10^{12}$	$1.15 \times 10^{15} \pm 2.30 \times 10^{13}$	$1.52 \times 10^{14} \pm 3.04 \times 10^{12}$	$1.23 \times 10^{15} \pm 2.46 \times 10^{13}$	$1.57 \times 10^{14} \pm 3.14 \times 10^{12}$	$1.02 \times 10^{15} \pm 2.04 \times 10^{13}$	$1.30 \times 10^{14} \pm 2.60 \times 10^{12}$
0.4	$1.39 \times 10^{14} \pm 2.78 \times 10^{12}$	$1.70 \times 10^{13} \pm 3.40 \times 10^{11}$	$1.28 \times 10^{14} \pm 2.56 \times 10^{12}$	$1.64 \times 10^{13} \pm 3.28 \times 10^{11}$	$1.49 \times 10^{14} \pm 2.98 \times 10^{12}$	$1.93 \times 10^{13} \pm 3.86 \times 10^{11}$	$1.24 \times 10^{14} \pm 2.48 \times 10^{12}$	$1.65 \times 10^{13} \pm 3.30 \times 10^{11}$
0.5	$2.23 \times 10^{13} \pm 6.69 \times 10^{11}$	$2.77 \times 10^{12} \pm 8.31 \times 10^{10}$	$1.91 \times 10^{13} \pm 5.73 \times 10^{11}$	$2.48 \times 10^{12} \pm 7.44 \times 10^{10}$	$2.24 \times 10^{13} \pm 6.72 \times 10^{11}$	$2.96 \times 10^{12} \pm 8.88 \times 10^{10}$	$2.06 \times 10^{13} \pm 6.18 \times 10^{11}$	$2.76 \times 10^{12} \pm 8.28 \times 10^{10}$
0.6	$7.57 \times 10^{12} \pm 2.27 \times 10^{11}$	$9.03 \times 10^{11} \pm 2.71 \times 10^{10}$	$6.35 \times 10^{12} \pm 1.91 \times 10^{11}$	$7.95 \times 10^{11} \pm 2.39 \times 10^{10}$	$7.16 \times 10^{12} \pm 2.14 \times 10^{11}$	$9.11 \times 10^{11} \pm 2.73 \times 10^{10}$	$6.86 \times 10^{12} \pm 2.06 \times 10^{11}$	$8.90 \times 10^{11} \pm 2.67 \times 10^{10}$
0.7	$5.00 \times 10^{12} \pm 2.00 \times 10^{11}$	$6.02 \times 10^{11} \pm 2.40 \times 10^{10}$	$4.64 \times 10^{12} \pm 1.86 \times 10^{11}$	$5.84 \times 10^{11} \pm 2.34 \times 10^{10}$	$4.56 \times 10^{12} \pm 1.82 \times 10^{11}$	$5.88 \times 10^{11} \pm 2.35 \times 10^{10}$	$4.64 \times 10^{12} \pm 1.85 \times 10^{11}$	$6.07 \times 10^{11} \pm 2.42 \times 10^{10}$
0.8	$3.90 \times 10^{14} \pm 1.56 \times 10^{13}$	$4.88 \times 10^{13} \pm 1.95 \times 10^{12}$	$3.25 \times 10^{14} \pm 1.30 \times 10^{13}$	$4.25 \times 10^{13} \pm 1.70 \times 10^{12}$	$3.13 \times 10^{14} \pm 1.25 \times 10^{13}$	$4.19 \times 10^{13} \pm 1.67 \times 10^{12}$	$4.91 \times 10^{14} \pm 1.96 \times 10^{13}$	$6.39 \times 10^{13} \pm 2.55 \times 10^{12}$
Average	$2.73 \times 10^{14}$	$3.32 \times 10^{13}$	$2.72 \times 10^{14}$	$3.56 \times 10^{13}$	$2.83 \times 10^{14}$	$3.65 \times 10^{13}$	$2.65 \times 10^{14}$	$3.45 \times 10^{13}$

by FWO method are higher compared to those obtained by KAS method. Despite differences among activation energies, they are not higher than 10% by which both calculations agree. Other authors have reported similar values of activation energy using the FWO method to be  $140.4 \text{ kJ mol}^{-1}$  in sewage sludge,  $143.3 \text{ kJ mol}^{-1}$  in animal manure, and  $173.9 \text{ kJ mol}^{-1}$  in the organic fraction of municipal solid waste [11]. By using the FWO method applied to pyrolysis of poplar wood, the average activation energy and frequency factor were  $158.6 \text{ kJ mol}^{-1}$  and  $7.96 \times 10^{13} \text{ min}^{-1}$ , whereas for KAS method, these values were  $157.3 \text{ kJ mol}^{-1}$  and  $1.69 \times 10^{13} \text{ min}^{-1}$ , respectively [4]. Values of activation energy and frequency factor obtained by the FWO method for torrefied stump chips were reported to be  $136.7 \text{ kJ mol}^{-1}$  and  $2.83 \times 10^9 \text{ s}^{-1}$ , respectively [55], which are similar to those reported for hazelnut husk using the FWO and KAS method to be  $131.1$  and  $127.8 \text{ kJ mol}^{-1}$  [25]. Using the FWO method, other authors [56] reported variations of activation energies ranging from  $143$  to  $268.7 \text{ kJ mol}^{-1}$  and frequency factors between  $1 \times 10^{12}$  to  $1 \times 10^{19} \text{ min}^{-1}$  while for *Acacia mangium* wood, values of activation energy and frequency factor were  $228.6 \text{ kJ mol}^{-1}$  and  $5.75 \times 10^8 \text{ s}^{-1}$  [7].

A similar comparison and analysis of results can be done for the Friedman method as shown in Fig. 4. Kinetic parameters obtained with fraction conversions from 0.2 to 0.7 are summarized in Table 4 where the average activation energy is  $174.2 \text{ kJ mol}^{-1}$  and the frequency factor is  $1.24 \times 10^{15} \text{ min}^{-1}$ . In addition, the regression equation is shown as well as its corresponding determination coefficient. It is observed that higher value of  $R^2$  is obtained for conversion values from 0.3 to 0.6. Conversions below than 0.2 and higher than 0.7 yielded poor linear fitting. Comparing the average activation energies obtained with the FWO, KAS, and Friedman method, discrepancies among these values are not higher than 10%.

Average value of activation energy by the Friedman method obtained in this study ( $174.2 \text{ kJ mol}^{-1}$ ) is like those obtained by other authors. For example, yellow poplar mixed with coking coal the activation energy diminished as biomass contents

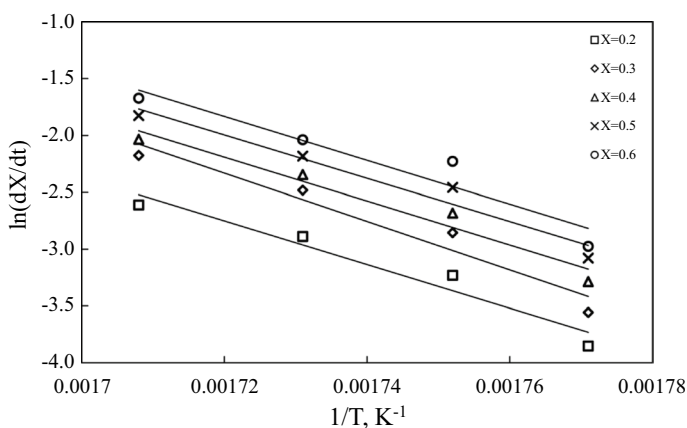


**Fig. 4** Kinetic calculations for differential method based on variable heating rates, i.e., 5, 10, 15, and  $20 \text{ }^\circ\text{C min}^{-1}$  under nitrogen atmosphere at  $50 \text{ cm}^3 \text{ min}^{-1}$ . Fractional conversion plotted was in the range from 0.2 to 0.6

increased in mixture and values of  $E_a$  ranged from 163.7 to 579.4 kJ mol<sup>-1</sup> as reported elsewhere [20]. White oak pyrolysis has been studied and activation energies values were calculated between 160 to 777 kJ mol<sup>-1</sup> for conversions between 5 and 80% [21]. Lower average activation energy for *Pinyon* pine was calculated to be 108 kJ mol<sup>-1</sup> [9]. Differences among activation energy calculated by the three methods in this study as function of conversion are plotted in Fig. 5. When comparing the average activation energy with literature reports in which pine or eucalyptus sawdust were used as feed using the Friedman, FWO, and KAS methods, the values respectively were: 126.6, 123.2, and 112.7 kJ mol<sup>-1</sup> for *Pinus pseudostrobus*; 148.1, 151.8, and 141.3 kJ mol<sup>-1</sup> for *Pinus leiophylla* [22]; 143, 136, and 133 kJ mol<sup>-1</sup> for *Eucalyptus benthamii*; 147.7, 140.5, and 137.5 kJ mol<sup>-1</sup> for *Eucalyptus dunnii*; 155.5, 147.9, and 145.2 kJ mol<sup>-1</sup> for *Pinus elliottii* [57]. In our study using *Pinus montezumae*, the average activation values for the aforementioned methods were: 174.2, 192.4, and 181.8 kJ mol<sup>-1</sup>. These values are higher than those reported in literature for other kind of pines, which is a consequence of the composition of sawdust and content of hemicellulose, cellulose, and lignin that influence on the rate of thermal degradation. Additionally, biomass commonly has low thermal conductivity enhancing large temperature gradients inside the particle by which reactions are carried out at different rates. Usually, activation energies ranging from 50 to 200 kJ mol<sup>-1</sup> are considered as acceptable values [58].

When assessing the three methods, it may be affirmed that the models used reveal that pyrolysis of the studied pinewood progresses through complex multiple kinetics. There are common aspects and some differences that allow suggesting these methods are useful for studying the behavior of the biomass during its pyrolytic decomposition. However, we consider that the FWO and KAS methods are the ones that provide the best and most complete information about the pyrolytic decomposition of pinewood due to the similarity of results as shown in Fig. 5. Because the biomass to be studied can come from older or younger trees, the FWO method may be considered more useful because it considers the reaction model, which is related to the different complexity degree of the wood structure as function of the strength of the polysaccharide-polysaccharide complexes formed through cellulose and hemicellulose constituents, which indeed is related to cellulose structure and its influence on the polymerization degree

**Table 4** Activation energy calculated by differential method at different conversion values

X	$E_a$ , kJ mol <sup>-1</sup>	Equation	R <sup>2</sup>	Frequency factor, min <sup>-1</sup>
0.2	159.5 ± 3.2	$y = -19181x + 30.239$	0.9457	$1.69 \times 10^{13} \pm 3.38 \times 10^{11}$
0.3	191.4 ± 3.8	$y = -23023x + 35.859$	0.9853	$5.35 \times 10^{15} \pm 1.07 \times 10^{14}$
0.4	168.5 ± 5.0	$y = -20269x + 30.502$	0.9912	$2.94 \times 10^{13} \pm 8.82 \times 10^{11}$
0.5	161.9 ± 4.9	$y = -19468x + 28.705$	0.9913	$5.85 \times 10^{12} \pm 1.76 \times 10^{11}$
0.6	165.9 ± 6.6	$y = -19952x + 29.078$	0.9958	$1.06 \times 10^{13} \pm 4.24 \times 10^{11}$
0.7	197.9 ± 7.9	$y = -23807x + 34.060$	0.8525	$2.06 \times 10^{15} \pm 8.24 \times 10^{13}$
Average	174.2			$1.24 \times 10^{15}$

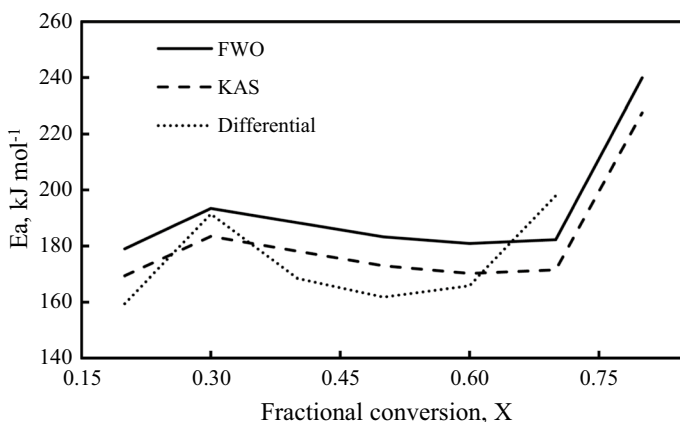


**Fig. 5** Activation energy as function of fractional conversion for different methods: FWO (solid line), KAS (dashed line), and differential method (dotted line). For FWO and KAS methods, fractional conversion plotted ranged from 0.2 to 0.8 while for differential method it was varied from 0.2 to 0.7. In all cases, nitrogen atmosphere at  $50 \text{ cm}^3 \text{ min}^{-1}$  from room temperature to  $800 \text{ }^\circ\text{C}$  were used for kinetic calculations with variations in heating rates ( $5, 10, 15,$  and  $20 \text{ }^\circ\text{C min}^{-1}$ )

and crystallinity thereof. Consequently, devolatilization of the cellulosic material varies depending on the age of the trees. The highest  $E_a$  values obtained by the FWO method, compared to those obtained by the KAS method as shown in Table 2, disclose the best information obtained by the first method about the reaction model mainly in the conversion values corresponding to the range of greatest degradation of hemicellulose, cellulose, and lignin (between  $250$  and  $350 \text{ }^\circ\text{C}$ ).

Mexico and Cuba also use forest biomass to obtain primary or secondary energy, depending on the different thermal conversion processes used, such as complete gasification (for obtaining fuel gas), combustion, and pyrolysis. The latter one is commonly used to obtain energy from carbon-based sources by which it is important to know how the activation energy values behave. These values are closely related to the complexity of chemical reactions and its kinetics due to the composition and structure of the wood constituents as explained.

## Conclusions

Kinetics of thermal decomposition of pine wood (*Pinus montezumae*) was studied by three methods. Decomposition was clearly observed from  $250$  to  $380 \text{ }^\circ\text{C}$  and mean activation energies and frequency factors calculated by FWO method were  $192.4 \text{ kJ mol}^{-1}$  and  $2.73 \times 10^{14} \text{ min}^{-1}$ , respectively, while for KAS method, the aforementioned values were  $181.8 \text{ kJ mol}^{-1}$  and  $3.32 \times 10^{13} \text{ min}^{-1}$ . On the other hand, mean activation energy calculated with the Friedman method was  $174.2 \text{ kJ mol}^{-1}$ . Three regions were observed during thermal decomposition of

pine sawdust regarding to water evaporation corresponding to 10% of weight loss followed by major changes due to decomposition of hemicellulose, cellulose, and partial degradation of lignin in the second stage, which represents almost 60% of weight loss of the pine sawdust, while the third stage occurred from 380 to 800 °C that corresponds to 10% of weight loss where lignin continued to be decomposed and residue is obtained. Differences in mean activation energies among the three methods were lower than 10% by which accurately predictions on activation energy are attained with all methods used. Activation energy computed by FWO method increased up to a fractional conversion of 0.3 to be 193.4 kJ mol<sup>-1</sup> to decrease steadily and finally increased again at fractional conversion higher than 0.7. Lower values of activation energy are observed for KAS method but showing similar trend compared to FWO, which indicates that higher reaction rate is obtained by KAS method. Increase of activation energy up to conversion of 30% is also observed by using the Friedman method followed by decreasing of  $E_a$  values and further increasing at conversions of 60–70%. At conversion values of 70%, the activation energy was the highest compared to FWO and KAS methods. Finally, the ratio of volatile mater-to-fixed carbon obtained from proximate analysis is 13.82, which may be considered as a high value indicating that most of compounds are converted into gases. The variation of  $E_a$  values observed between the three methods provides information about the complexity of the structure of the polymeric substances present in the studied material. For this reason, the results obtained are of great importance to determine the production parameters of energy in the scaling stage in Mexico and Cuba, from biomass coming from *Pinus montezumae*.

**Acknowledgements** Authors thank to Centro Latinoamericano de Física (CLAF) and Secretaría de Ciencia, Tecnología e Innovación (SECITI) from the Mexico City Government for financial support. Authors acknowledge Laboratorio Nacional de Conversión y Almacenamiento de Energía (LNCAE) for access to its experimental facility.

## References

1. Grasi G (1989) Pyrolysis and gasification of biomass. In: Ferrero GL, Maniatis K, Buekens A, Bridgwater AV (eds) Pyrolysis and gasification. Elsevier Applied Sciences, London
2. Beenackers AACM, Bridgwater AV (1989) Pyrolysis and gasification 1. Elsevier Applied Sciences, London
3. Hastouglu MA, Hassam MS (1995) Application of general gas-solid reaction model to flash pyrolysis of wood in a circulation fluidized bed. Fuel 74:697–703. [https://doi.org/10.1016/0016-2361\(94\)00010-0](https://doi.org/10.1016/0016-2361(94)00010-0)
4. Słopiecka K, Bartocci P, Fantozzi F (2012) Thermogravimetric analysis and kinetic study of poplar wood pyrolysis. Appl Energy 97:491–497. <https://doi.org/10.1016/j.apenergy.2011.12.056>
5. García-Rojas LM, Márquez-Montesino F, Aguiar-Trujillo L, Arauso-Pérez J, Carballo-Abreu LR, Orea-Igarza U, Zanzi R (2009) Rendimiento de los productos de la descomposición térmica de la madera de *Eucalyptus saligna* Smith a diferentes alturas del fuste comercial. Rev Chapingo Ser Cie 15:147–154
6. Correa F, González M, Servín H, Márquez F, Rutiaga JG, Lemus AA, Reguera E, Alonso V (2014) Development of a selective low cost absorbing surface based on soot for solar thermal applications. Energy Proc 57:1565–1572. <https://doi.org/10.1016/j.egypro.2014.10.148>

7. Márquez-Montesino F, Correa-Méndez F, Glauco-Sánchez C, Zanzi-Vigouroux R, Rutiaga-Quiñones JG, Aguiar-Trujillo L (2015) Pyrolytic degradation studies of Acacia magnium wood. *BioResources* 10:1825–1844. <https://doi.org/10.15376/biores.10.1.1825-1844>
8. Masnadi MS, Habibi R, Kopyscinski J, Hill JM, Bi X, Lim CJ, Ellis N, Grace JF (2014) Fuel characterization and co-pyrolysis kinetics of biomass and fossil fuels. *Fuel* 117:1204–1214. <https://doi.org/10.1016/j.fuel.2013.02.006>
9. Kim SS, Shenoy A, Agblevor FA (2014) Thermogravimetric and kinetic study of *Pinyon* pine in the various gases. *Bioresour Technol* 156:297–302. <https://doi.org/10.1016/j.biortech.2014.01.066>
10. Shadangi KP, Mohanty K (2014) Kinetic study and thermal analysis of the pyrolysis of non-edible oilseed powders by thermogravimetric and differential scanning calorimetric analysis. *Renew Energy* 63:337–344. <https://doi.org/10.1016/j.renene.2013.09.039>
11. Sánchez ME, Otero M, Gómez X, Morán A (2009) Thermogravimetric kinetic analysis of the combustion of biowastes. *Renew Energy* 34:1622–1627. <https://doi.org/10.1016/j.renene.2008.11.011>
12. El-Sayed SA, Mostafa ME (2014) Pyrolysis characteristics and kinetic parameters determination of biomass fuel powders by differential thermal gravimetric analysis (TGA/DTG). *Energy Convers Manage* 85:165–172. <https://doi.org/10.1016/j.enconman.2014.05.068>
13. Gai C, Dong Y, Zhang T (2012) The kinetic analysis of the pyrolysis of agricultural residue under non-isothermal conditions. *Bioresour Technol* 127:298–305. <https://doi.org/10.1016/j.biortech.2012.09.089>
14. Sarkar JK, Wang Q (2020) Characterization of pyrolysis products and kinetic analysis of waste jute stick biomass. *Processes* 8:837. <https://doi.org/10.3390/pr8070837>
15. Skodras G, Grammelis P, Basinas P, Kaldis S, Kakaras E, Sakellariopoulos GP (2006) A kinetic study on the devolatilisation of animal derived byproducts. *Fuel Process Technol* 88:787–794. <https://doi.org/10.1016/j.fuproc.2007.03.009>
16. Edreis EMA, Luo G, Yao H (2014) Investigations of the structure and thermal kinetic analysis of sugarcane bagasse char during non-isothermal CO<sub>2</sub> gasification. *J Anal Appl Pyrol* 107:107–115. <https://doi.org/10.1016/j.jaap.2014.02.010>
17. García-Barneto A, Ariza-Carmona J, Conesa-Ferrer JA, Díaz-Blanco MJ (2010) Kinetic study on the thermal degradation of a biomass and its compost: composting effect on hydrogen production. *Fuel* 89:462–473. <https://doi.org/10.1016/j.fuel.2009.09.024>
18. Syed S, Qudaih R, Talab I, Janajreh I (2011) Kinetics of pyrolysis and combustion of oil shale sample from thermogravimetric data. *Fuel* 90:1631–1637. <https://doi.org/10.1016/j.fuel.2010.10.033>
19. Gangavati PB, Safi MJ, Singh A, Prasad B, Mishra IM (2005) Pyrolysis and thermal oxidation kinetics of sugar mill press mud. *Thermochim Acta* 428:63–70. <https://doi.org/10.1016/j.tca.2004.09.026>
20. Jeong MH, Seo WM, Jeong SM, Na BK, Yoon SJ, Lee JG, Lee WJ (2014) Pyrolysis kinetics of coking coal mixed with biomass under non-isothermal and isothermal conditions. *Bioresour Technol* 155:442–445. <https://doi.org/10.1016/j.biortech.2014.01.005>
21. Park HJ, Park YK, Dong JI, Kim JS, Jeon JK, Kim SS, Kim J, Song B, Park J, Lee KJ (2009) Pyrolysis characteristic of Oriental white oak: kinetic study and fast pyrolysis in a fluidized bed with an improved reaction system. *Fuel Process Technol* 90:186–195. <https://doi.org/10.1016/j.fuproc.2008.08.017>
22. Alvarado-Flores JJ, Rutiaga-Quiñones JG, Ávalos-Rodríguez ML, Alcaraz-Vera JV, Espino-Valencia J, Guevara-Martínez SJ, Márquez-Montesino F, Alfaro-Rosas A (2020) Thermal degradation kinetics and FR-IR análisis on the pyrolysis of *Pinus pseudostrobus*, *Pinus leiophylla* and *Pinus montezumae* as forest waste in Western Mexico. *Energies* 13:969. <https://doi.org/10.3390/en13040969>
23. Han S, Jang Y-C, Choi Y-S, Choi S-K (2020) Thermogravimetric kinetic study of automobile shredder residue (ASR) pyrolysis. *Energies* 13:1451. <https://doi.org/10.3390/en13061451>
24. Hu S, Jess A, Xu M (2007) Kinetics study of Chinese biomass slow pyrolysis: comparison of different kinetic models. *Fuel* 86:2778–2788. <https://doi.org/10.1016/j.fuel.2007.02.031>
25. Ceylan S, Topçu Y (2014) Pyrolysis kinetics of hazelnut husk using thermogravimetric analysis. *Bioresour Technol* 156:182–188. <https://doi.org/10.1016/j.biortech.2014.01.040>
26. Lyon RE (1997) An integral method of nonisothermal kinetic analysis. *Thermochim Acta* 297:117–124. [https://doi.org/10.1016/S0040-6031\(97\)00158-5](https://doi.org/10.1016/S0040-6031(97)00158-5)
27. ASTM D 1106–96 (2007) Standard test method for acid-insoluble lignin in wood. ASTM International
28. TAPPI Test Method T 203 cm-99 (1999) Alpha-, beta- and gamma-cellulose in pulp. TAPPI Press
29. ASTM D 1104–78 (1978) Standard test method for holocellulose in wood. ASTM International



30. ASTM D 4442–07 (2007) Standard test methods for direct moisture content measurement of wood and wood-base materials. ASTM International
31. ASTM D 1102–84 (2007) Standard test method for ash in wood. ASTM International
32. ASTM D 3175–07 (2007) Standard method for volatile matter in the analysis sample of char and coke. ASTM International
33. Márquez-Montesino F, Cordero-Alcántara T, Rodríguez-Mirasol J, Rodríguez-Jiménez JJ (2001) Estudio del potencial energético de biomasa *Pinus caribaea* Morelet var. *Caribaea* (Pc) y *Pinus tropicalis* Morelet (Pt); *Eucalyptus saligna* Smith (Es), *Eucalyptus citriodora* Hook (Ec) y *Eucalyptus pellita* F.(Muell) (Ep); de la Provincia de Pinar del Río. Rev Chapingo Ser Cie 7:83–89
34. Márquez-Montesino F, Carballo-Abreu LR, Álvarez-Olivera PA, Castillo-Ramos R (2009) I. Study of the energy possibilities of the wood of Jambolán (*Syzygium cumini*), of the municipality of Pinar del Río, Cuba. Advances CIGET 11:July-September
35. Aguiar L, Márquez-Montesinos F, Gonzalo A, Sánchez JL, Arauzo J (2008) Influence of temperature and particle size on the fixed bed pyrolysis of orange peel residues. J Anal Appl Pyrol 83:124–130. <https://doi.org/10.1016/j.jaap.2008.06.009>
36. Rosas JM, Bedia J, Rodríguez-Mirasol J, Cordero R (2009) HEMP-derived activated carbon fibers by chemical activation with phosphoric acid. Fuel 88:19–26. <https://doi.org/10.1016/j.fuel.2008.08.004>
37. Azharul Islam Md, Asif M, Hameed BH (2015) Pyrolysis kinetics of raw and hydrothermally carbonized Karanj (*Pongamia pinnata*) fruit hulls via thermogravimetric analysis. Bioresour Technol 179:227–233. <https://doi.org/10.1016/j.biortech.2014.11.115>
38. Aguado R, Olazar M, Gaisán B, Prieto R, Bilbao J (2002) Kinetic study of polyolefin pyrolysis in a conical spouted bed reactor. Ind Eng Chem Res 41:4559–4566. <https://doi.org/10.1021/ie0201260>
39. Shen DK, Gu S, Luo KH, Bridgwater AV, Fang MX (2009) Kinetic study on thermal decomposition of woods in oxidative environment. Fuel 88:1024–1030. <https://doi.org/10.1016/j.fuel.2008.10.034>
40. Moghadam RA, Yusup S, Uemura Y, Chin BLG, Lam HL, Al Shoaibi A (2014) Syngas production from palm kernel shell and polyethylene waste blend in fluidized bed catalytic steam co-gasification process. Energy 75:40–44. <https://doi.org/10.1016/j.energy.2014.04.062>
41. Balat M, Balat M, Kirtay E, Balat H (2009) Main routes for the thermo-conversion of biomass into fuels and chemicals. Part 1: pyrolysis systems. Energy Convers Manage 50:3147–3157. <https://doi.org/10.1016/j.enconman.2009.08.014>
42. Fisher T, Hajjalilgol M, Waymack B, Kellogg D (2002) Pyrolysis behavior and kinetics of biomass derived materials. J Anal Appl Pyrol 62:331–349. [https://doi.org/10.1016/S0165-2370\(01\)00129-2](https://doi.org/10.1016/S0165-2370(01)00129-2)
43. Jiang H, Cheng Z, Zhao T, Liu M, Zhang M, Li J, Hu M, Zhang L, Li J (2014) Pyrolysis kinetics of spent lark mushroom substrate and characterization bio-oil obtained from the substrate. Energy Convers Manage 88:259–266. <https://doi.org/10.1016/j.enconman.2014.08.006>
44. Maiti S, Purakayastha S, Ghosh B (2007) Thermal characterization of mustard straw and stalk in nitrogen at different heating rates. Fuel 86:1513–1518. <https://doi.org/10.1016/j.fuel.2006.11.016>
45. Hayashi J, Horikawa T, Takeda I, Muroyama K, Ani FN (2002) Preparing activated carbon from various nutshells by chemical activation with  $K_2CO_3$ . Carbon 40:2381–2386. [https://doi.org/10.1016/S0008-6223\(02\)00118-5](https://doi.org/10.1016/S0008-6223(02)00118-5)
46. Jung SH, Oh SJ, Choi GG, Kim JS (2014) Production and characterization of microporous activated carbons and metallurgical bio-coke from waste shell biomass. J Anal Appl Pyrol 109:123–131. <https://doi.org/10.1016/j.jaap.2014.07.003>
47. Yang X, Zhang R, Fu J, Geng S, Cheng JJ, Sun Y (2014) Pyrolysis kinetic and product analysis of different microalgal biomass by distributed activation energy model and pyrolysis–gas chromatography–mass spectrometry. Bioresour Technol 163:335–342. <https://doi.org/10.1016/j.biortech.2014.04.040>
48. Corbetta M, Frassoldati A, Bennadji H, Smith K, Serapiglia MJ, Gauthier G, Melkior T, Ranzi E, Fisher EM (2014) Pyrolysis of centimeter-scale woody biomass particles: kinetic modeling and experimental validation. Energy Fuel 28:3884–3898. <https://doi.org/10.1021/ef500525v>
49. Saffe A, Fernández A, Echegaray M, Mazza G, Rodríguez R (2019) Pyrolysis kinetics of regional agro-industrial wastes using isoconversional methods. Biofuels 10:245–257. <https://doi.org/10.1080/17597269.2017.1316144>
50. Channiwala S, Parikh P (2002) A unified correlation for estimating HHV of solid, liquid and gaseous fuels. Fuel 81:1051–1063. [https://doi.org/10.1016/S0016-2361\(01\)00131-4](https://doi.org/10.1016/S0016-2361(01)00131-4)
51. Pandey MP, Kim CS (2011) Lignin depolymerization and conversion: a review of thermochemical methods. Chem Eng Technol 34:29–41. <https://doi.org/10.1002/ceat.201000270>

52. Nunes CA, Lima CF, Barbosa LCA, Colodetter JL, Gouveia AFG, Silvério FO (2010) Determination of *Eucalyptus* spp. lignin S/G ratio: a comparison between methods. *Bioresour Technol* 101:4056–4061. <https://doi.org/10.1016/j.biortech.2010.01.012>
53. Mohamed AR, Hamzah Z (2015) An alternative approach for the screening of catalytic empty fruit bunch (EFB) pyrolysis using the values of activation energy from a thermogravimetric study. *Reac Kinet Mech Cat* 114:529–545. <https://doi.org/10.1007/s11144-014-0798-8>
54. Li L, Rowbotham JS, Greenwell HC, Dyer PW (2013) An introduction to pyrolysis and catalytic pyrolysis: versatile techniques for biomass conversion. In: Suib SL (ed) *New and future developments in catalysis*. Elsevier, Amsterdam
55. Tran KQ, Bach QV, Trinh TT, Seisenbaeva G (2014) Non-isothermal pyrolysis of torrefied stump—a comparative kinetic evaluation. *Appl Energy* 136:759–766. <https://doi.org/10.1016/j.apenergy.2014.08.026>
56. Wu K, Liu J, Wu Y, Chen Y, Li Q, Xiao X, Yang M (2014) Pyrolysis characteristics and kinetics of aquatic biomass using thermogravimetric analyzer. *Bioresour Technol* 163:18–25. <https://doi.org/10.1016/j.biortech.2014.03.162>
57. Gomes da Silva JC, Alves JLF, de Araujo Galdino WV, Floriani Andersen SL, de Sena RF (2018) Pyrolysis kinetic evaluation by single-step for waste wood from reforestation. *Waste Manage* 72:265–273. <https://doi.org/10.1016/j.wasman.2017.11.034>
58. Subramanian S, Ragula UBR (2018) Pyrolysis kinetics of *Hibiscus rosa sinensis* and *Nerium oleander*. *Biofuels*. <https://doi.org/10.1080/17597269.2018.1432274>

**Publisher's Note** Springer Nature remains neutral with regard to jurisdictional claims in published maps and institutional affiliations.